Pergamon

Tetrahedron, Vol. 53, No. 1, pp. 59-72, 1997

0040-4020/97 $17.00 + 0.00

PII: S0040-4020(96)00978-7

Novel Mammalian Cell Cycle Inhibitors, Cyclotryprostatins A-D, Produced by *Aspergillus fumigatus*, Which Inhibit Mammalian Cell Cycle at G2/M Phase

Cheng-Bin Cui, Hideaki Kakeya and Hiroyuki Osada*

The Institute of Physical and Chemical Research (RIKEN),
Hirosawa 2-1, Wako-shi 351-01, Saitama, Japan

Abstract: Four new natural diketopiperazine derivatives, cyclotryprostatins A (**1**), B (**2**), C (**3**) and D (**4**), were isolated as new inhibitors of the mammalian cell cycle from the secondary metabolites of *Aspergillus fumigatus* BM939 through a separation procedure guided by cell cycle inhibitory activity. The structures of **1**-**4** were determined by spectroscopic methods especially by detailed analyses of their ^{1}H and ^{13}C NMR spectra with the aid of 2D NMR techniques. Compounds **1**-**4** inhibited the cell cycle progression of tsFT210 cells at the G2/M phase with IC_{50} values of 5.6 μM (**1**), 19.5 μM (**2**), 23.4 μM (**3**) and 25.3 μM (**4**), respectively. Copyright © 1996 Elsevier Science Ltd

In the course of our screening for new cell cycle inhibitors from microbial origin[1-7], which might be good candidates for cancer chemotherapy and also be a source for providing molecular probes useful in elucidating regulatory mechanism of the cell cycle, we have previously reported novel diketopiperazine derivatives, tryprostatins[2,4,5] A, B and spirotryprostatins[6,7] A, B as well as a new natural diketopiperazine derivative, demethoxyfumitremorgin C[4,5], together with four known diketopiperazines[4,5], fumitremorgin C, 12,13-dihydroxyfumitremorgin C, fumitremorgin B and verruculogen, as a new group of G2/M-phase inhibitors of the mammalian cell cycle, which were isolated from the fermentation broth of a fungus, *Aspergillus fumigatus* BM939[2-7].

In the continuation of that work, we have recently isolated four new natural diketopiperazine derivatives, cyclotryprostatins A (**1**), B (**2**), C (**3**) and D (**4**) (Chart 1), from the fermentation broth of *Aspergillus fumigatus* BM939 through a separation procedure guided by inhibitory activity on the cell cycle progression of

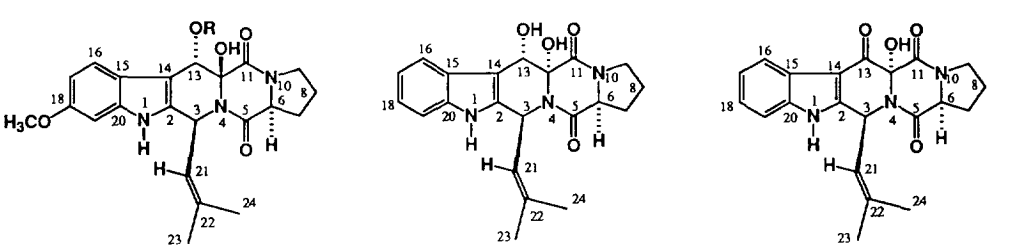

1 : R = H
2 : R = CH_3

3

4

Chart 1 Structures of Cyclotryprostatins A (**1**), B (**2**), C (**3**) and D (**4**).

mouse tsFT210 cells. Cyclotryprostatins A (**1**)-D (**4**) inhibited the cell cycle progression of tsFT210 cells at the G2/M phase and were named according to their structural and biological relations to tryprostatins. We describe herein the isolation, structure determination and biological activities of **1**-**4**.

Fermentation and Isolation

The producing strain was cultured in a 600-liter jar fermenter containing 400 liters of fermentation medium (glucose 3%, soluble starch 2%, soybean meal 2%, K_2HPO_4 0.5% and $MgSO_4 \cdot 7H_2O$ 0.05%, adjusted at pH 6.5 before sterilization) containing 0.05% of CA-123 and KM-68 antifoam, respectively. The fermentation was carried out at 28°C for 66 hours under 350 rpm stirring speed and 200 liters/minute aeration rate.

The whole broth was filtrated to obtain a broth supernatant (370 L) and a mycelial cake. The latter was extracted with 90% aqueous acetone which was evaporated *in vacuo* to give an aqueous solution (60 L). Both the aqueous solution and the broth supernatant were extracted respectively with EtOAc. The EtOAc solutions obtained were combined and concentrated *in vacuo* to afford an oily extract (1.2 L) which was further purified as shown in Fig. 1 to give an active extract (66 g). This extract was then separated by a combination of silica gel column chromatography and repeated HPLC (CAPCELL PAK C-18 and CAPCELL PAK C-8, Shiseido) to give **1** (1 mg), **2** (4.4 mg), **3** (12.4 mg) and **4** (1.2 mg), respectively (Fig. 1).

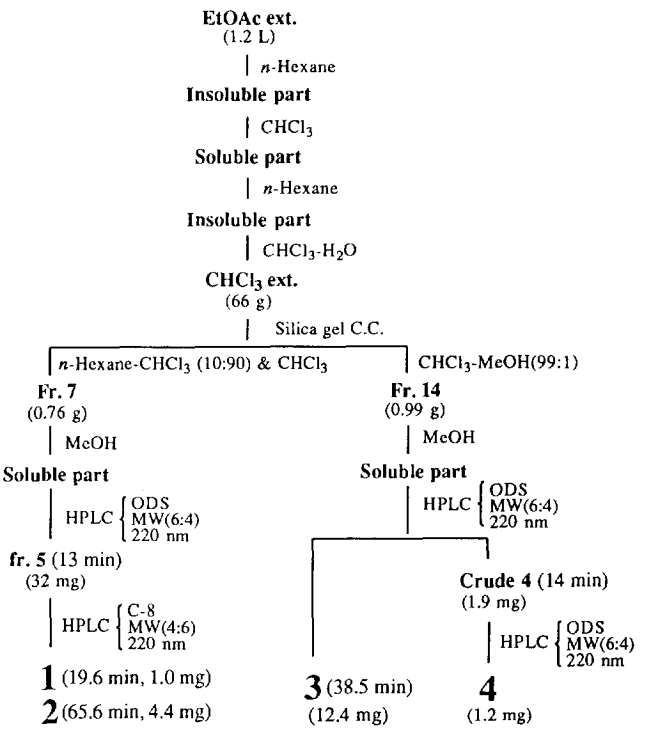

Fig. 1. Isolation Procedure for Cyclotryprostatins A (**1**)-D (**4**).
MW is the abbreviation of MeOH-Water.

Physico-chemical Properties of Cyclotyprostatins A (1)-D (4)

Cyclotryprostatins A (**1**)-D (**4**) were obtained as slightly yellow-colored forms or crystals and their

physico-chemical properties are summarized in Table 1.

Table 1. Physico-chemical Properties of Cyclotryprostatins A (**1**), B (**2**), C (**3**), and D (**4**).

Characteristics	**1**	**2**	**3**	**4**
Appearance	Pale Yellow Crystalline Powder	Pale Yellow Crystalline Solid	White Needles	Pale Yellow Amorphous Powder
MP	180-185°C (dec.)	159-165°C (dec.)	221-223°C (dec.)	——
$[\alpha]_D$ in $CHCl_3$	$[\alpha]_D^{23}$ +104.3°(c 0.07)	$[\alpha]_D^{24}$ +95.7°(c 0.36)	$[\alpha]_D^{25}$ +23.4°(c 1.0)	$[\alpha]_D^{26}$ +88.0°(c 0.10)
Molecular Formular	$C_{22}H_{25}N_3O_5$	$C_{23}H_{27}N_3O_5$	$C_{21}H_{23}N_3O_4$	$C_{21}H_{21}N_3O_4$
Molecular Weight	411	425	381	379
EI-MS *m/z*	411 (M^+, 79%), 243 (62%), 200 (100%)	425 (M^+, 94%), 257 (100%), 226 (56%)	381 (M^+, 27%), 364 (11%), 213 (100%), 170 (40%), 157 (57%)	379 (M^+, 18%), 211 (100%)
HR-EI-MS	M^+	M^+	M^+	M^+
Found (*m/z*)	411.1765	425.1944	381.1693	379.1472
Calcd (*m/z*)	411.1768	425.1944	381.1694	379.1466
UV λ_{max}^{MeOH} nm (ε)	226 (27660), 259 (7230), 265sh (6860), 294 (7070), 303sh (5510)	224 (41690), 262 (7180), 267 (7180), 295 (8290), 303sh (6590)	224 (19680), 272 (6570), 280sh (6325), 290sh (5220)	216 (18290), 240sh (12320), 247 (15310), 264 (9720), 267sh (9570), 301 (8550)
IR ν_{max}^{KBr} cm^{-1}	3410, 3300 (OH & NH), 2970, 2930, 2870, 2855 (CH_3 & CH_2), 1665, 1655 (amide C=O), 1640 (C=C), 1460, 1430, 1160, 1030, 945, 830	3410, 3320 (OH & NH), 2970, 2930, 2870, 2830 (CH_3 & CH_2), 1670, 1650 (amide C=O), 1635 (C=C), 1460, 1415, 1160, 1080, 955, 830	3470, 3420, 3280 (OH & NH), 2970, 2930, 2870, 2860 (CH_3 & CH_2), 1680, 1665 (amide C=O), 1478, 1452, 1378, 745	3380, 3260 (OH & NH), 2970, 2930, 2880, 2860 (CH_3 & CH_2),1695 (conj. C=O), 1685, 1650 (amide C=O), 1455, 1375, 1360, 755

Planar Structures of Cyclotryprostatin A (1)-D (4)

Cyclotryprostatin A (**1**), $[\alpha]_D$ +104.3° ($CHCl_3$), was obtained as a pale yellow crystalline powder having melting point of 180-185°C (dec.) and had the molecular formula $C_{22}H_{25}N_3O_5$ determined by HR-EI-MS measurement (Table 1). In the UV spectrum, **1** showed characteristic absorption curve suggestive of a 6-*O*-methylindole chromophore with absorption maxima at 226 (ε 27660), 259 (7230), 265sh (6860), 294 (7070) and 303sh nm (5510)[2,5,8], and the IR spectrum of **1** showed absorption bands at 3410, 3300 (OH and NH), 2970, 2930, 2870, 2855 (CH_3 and CH_2), 1665 and 1655 cm^{-1} (amide C=O) in the functional group region.

In the ^1H NMR spectrum, **1** showed signals due to an N-H proton (δ7.83 br s, 1-H), a 1,2,4-trisubstituted

benzene ring (δ7.45 d, *J*=8.5 Hz, 16-H; δ6.81 dd, *J*= 8.5, 2.1 Hz, 17-H; and δ6.86 d, *J*=2.1 Hz, 19-H) and a methoxy (δ3.82 s, $OC\underline{H}_3$) and two methyl (δ1.79 s, 23-$\underline{H}_3$ and δ2.04 s, 24-$\underline{H}_3$) groups along with signals due to several methine and methylene groups (Table 2). The ^{13}C NMR spectrum of **1**, analyzed by the DEPT method, indicated the presence of two amide carbonyls (δ165.55 s, C-5 and δ166.87 s, C-11), an oxygen-bearing sp^2 carbon (δ156.72 s, C-18) and a methoxy (δ55.73 q, $O\underline{C}H_3$) and two methyl (δ26.05 q, C-23 and δ18.29 q, C-24) groups together with four sp^2 and three sp^3 methines, five sp^2 and a sp^3 quaternary carbons, and three methylene groups (Table 2).

The amide carbonyl absorption at 1665 and 1655 cm^{-1} together with the absence of the amide II band near 1550 cm^{-1} in the IR spectrum suggested the presence of a diketopiperazine system[2,5,9-11] in **1**. This was further supported by the amide carbonyl carbon signals at δ165.55 and δ166.87 (C-5 and C-11) in the ^{13}C NMR spectrum, which were assignable to the carbonyls in the diketopiperazine part[2,5-7].

Detailed analyses of the ^1H and ^{13}C NMR spectra (Table 2) of **1** with the aid of ^1H-^1H COSY and pulse field gradient heteronuclear multiple quantum coherence (PFG-HMQC) spectroscopy, coupled with the results of difference NOE experiments (Table 2) and the above structural information, led us to consider that the structure of **1** is composed from a 6-*O*-methylindole moiety, a diketopiperazine part and an isoprenyl residue, forming a pentacyclic ring skeleton.

The above structural units associated with the proton spin systems and the through-space interactions in **1** were confirmed by the structural information from the PFG heteronuclear multiple bond correlation (PFG-HMBC) spectrum (Table 2). For instance, the oxygen-bearing sp^2 quaternary carbon C-18 (δ156.72) and the sp^2 quaternary carbons C-20 (δ136.76) and C-15 (δ120.57) in the *O*-methylindole moiety in **1** could be assigned according to the long-range correlations between C-18 and the protons 16-H, 17-H, and 19-H, between C-20 and the protons 1-H, 16-H and 19-H, and between C-15 and the protons 1-H, 17-H and 19-H, respectively, and the methoxy (δ_H3.82 and δ_C55.73) was linked to C-18 according to the long-range correlation of the methoxy protons (δ3.82) with C-18 in the PFG-HMBC spectrum. Similarly, the quaternary carbons C-14 (δ107.41) and C-2 (δ133.34) in the same structural unit could be assigned on the basis of the long-range correlations, the former C-14 with 1-H and 16-H and the latter C-2 with 1-H, respectively, in the PFG-HMBC spectrum. Thus the methoxyindole moiety in **1** was confirmed. Also, the other long-range correlations confirming the isoprenyl residue and the diketopiperazine part in **1** are given in Table 2.

The connectivities between those structural units were determined by detailed analysis of the PFG-HMBC spectrum (Table 2). Both 3-H in the isoprenyl residue and 13-H neighbored to C-12 to form the diketopiperazine part in **1**, for example, showed long-range correlations with the carbons C-2, C-14 (in the methoxyindole moiety) and C-12 (in the diketopiperazine part). The former 3-H and the latter 13-H correlated further with C-5 in the diketopiperazine part and with C-15 in the methoxyindole moiety, respectively, in the PFG-HMBC spectrum. Those data evidenced the connectivity between the above structural units to form a central heterocyclic ring in **1**. Some other long-range correlations detected in the PFG-HMBC spectrum are summarized in Table 2, which evidenced also the connectivities between the structural units in **1** and thus the planar structure of **1** was deduced.

Cyclotryprostatin B (**2**) was obtained as a pale yellow crystalline solid having melting point of 159-165°C (dec.) and showed $[\alpha]_D$ +95.7° ($CHCl_3$). The molecular formula of **2** was determined to be $C_{23}H_{27}N_3O_5$ by HR-EI-MS measurement (Table 1), which is CH_2 more than that of **1**. The UV and IR spectra (Table 1) of **2** respectively suggested, like those of **1**, the presence of a 6-*O*-methylindole chromophore and a diketopiperazine system in **2**. The ^1H and ^{13}C NMR spectra of **2** closely resembled those of **1**, except for the appearance of additional methoxy signals (δ_H3.36 s and δ_C56.59 q) and the slight changes in the chemical shifts of several

Table 2. 500 MHz ^1H and 125 MHz ^{13}C NMR data for **1** and **2** in chloroform-d[a)]

Positions	1				2			
	δ_H (J in Hz)	NOEs[b)]	δ_c	HMBC[c)]	δ_H (J in Hz)	NOEs[b)]	δ_c	HMBC[c)]
1 (N<u>H</u>)	7.83 br s	3, 19	--------		7.86 br s	3, 19, 21	-------	
2	-----		133.34 s	1, 3, 13	-----		133.65 s	1, 3, 13
3	6.65 d (9.8)	1, 24	48.86 d		6.64 d (9.8)	1, 21, 24	49.06 d	
5	-----		165.55 s	3, 6, 7β	-----		167.02 s	3, 6
6	4.42 dd (10.5, 6.1)	7α	60.10 d		4.375 dd (10.7, 6.4)	7α	59.98 d	
7α	2.49 m	6, 7β, 8α	29.86 t	6	2.49 m	6, 7β, 8α	29.68 t	6
β	1.99 m				2.00 m			
8α	1.99 m		22.07 t	7α, 7β	2.00 m		22.11 t	7β
β	2.10 m				2.11 m			
9	3.76 m		45.85 t	7α	3.75 m		45.81 t	7α
	3.66 m				3.70 m			
11	-----		166.87 s		-----		165.84 s	13[d)]
12	-----		85.51 s	3, 13	-----		84.68 s	3, 13
13	5.09 s	16	68.88 d		4.74 s	13-OC<u>H</u>$_3$, 16	76.76 d	13-OC<u>H</u>$_3$
14	-----		107.41 s	1, 3, 13, 16	-----		105.29 s	1, 3, 13, 16
15	-----		120.57 s	1, 13, 17, 19	-----		122.59 s	1,13,16,17,19
16	7.45 d (8.5)	13, 17	118.42 d		7.44 d (8.6)	13, 17	118.63 d	
17	6.81 dd (8.5, 2.1)	16,18-OC<u>H</u>$_3$	109.97 d	19	6.82 dd (8.6, 2.2)	16, 18-OC<u>H</u>$_3$	110.01 d	19
18	-----		156.72 s	16,17,18-OC<u>H</u>$_3$,19	-----		156.45 s	16,17,18-OC<u>H</u>$_3$,19
19	6.86 d (2.1)	1,18-OC<u>H</u>$_3$	95.26 d	17	6.88 d (2.2)	1, 18-OC<u>H</u>$_3$	95.18 d	17
20	-----		136.76 s	1, 16, 19	-----		136.59 s	1, 16, 19
21	5.60 dm (9.8)	3, 23	123.35 d	3, 23, 24	5.56 dm (9.8)	3, 23	123.52 d	3, 23, 24
22	-----		138.12 s	3, 23, 24	-----		137.91 s	3, 23, 24
23	1.79[e)] s	21, 24	26.05 q	21, 24	1.79[e)] d (0.98)	21, 24	26.07 q	21, 24
24	2.04[f)] s	3, 23	18.29 q	21, 23	2.05[f)] d (1.46)	3, 23	18.23 q	21, 23
12-O<u>H</u>	4.44 br s	13	--------		4.38 br s	13	--------	
13-O<u>H</u>	2.21 br s		--------		-----		--------	
13-OCH$_3$	-----		--------		3.36 s	6, 13, 16	56.59 q	13
18-OCH$_3$	3.82 s	17, 19	55.73 q		3.83 s	17, 19	55.73 q	

a): Signal assignments were based on the results of ^1H-^1H COSY, PFG-HMQC, PFG-HMBC and difference NOE experiments. b): Numbers in the column indicate the protons on where NOEs were observed in the difference NOE experiments under irradiation at the proton in the corresponding line. c): Numbers in the column indicate the protons coupled with the carbon through two or three bonds, respectively, which were detected in the PFG-HMBC spectra measured with long-range J_{CH} values of 2.8 Hz for **1** (sample 1 mg, 96 scans) and 8.3 Hz or 4 Hz for **2** (sample 4.4 mg, 48 or 24 scans), respectively. d): The proton was detected in the PFG-HMBC spectrum measured with the long-range J_{CH} value of 4 Hz (sample 4.4 mg, 24 scans). e) and f): Long-range ^1H-^1H couplings were observed both with 21-H and with each other, respectively, in each sample in the ^1H-^1H COSYs.

proton and carbon signals (Table 2).

Those structural information revealed that **2** may be an *O*-methyl derivative of **1** and this was confirmed by extensive analyses of its ^{1}H-^{1}H COSY, PFG-HMQC and PFG-HMBC spectra (Table 2). The location of the additional methoxy group (δ_H3.36 and δ_C56.59, 13-OCH_3) in **2** at C-13 was determined by the long-range correlation of the methoxy protons (δ3.36) with C-13, in the PFG-HMBC spectrum (Table 2). Thus the planar structure of **2** was determined.

Cyclotryprostatin C (**3**), white needles, mp 221-223°C (dec.), showed $[\alpha]_D$ +23.4° ($CHCl_3$) and its molecular formula $C_{21}H_{23}N_3O_4$ (Table 1) is CH_2O less than that of **1**. The UV spectrum of **3** showed typical absorption pattern of the indole chromophore with absorption maxima at 224 (ε 19680), 272 (6570), 280sh (6325) and 290sh nm (5220)[2,5,8,10], and the IR spectrum suggested, like those of **1** and **2**, the presence of a diketopiperazine system in **3** (Table 1). Those data revealed that **3** may be a demethoxy derivative of **1**.

The ^{1}H and ^{13}C NMR spectra of **3**, extensively analyzed with the aid of ^{1}H-^{1}H COSY, DEPT and PFG-HMQC methods, indicated the presence of an N-H proton (δ7.91 br s, 1-H), a 1,2-disubstituted benzene ring (δ_H7.94 br d, *J*=7.8 Hz, 16-H; δ_H7.13 br t, *J*=7.8 Hz, 17-H; δ_H7.18 td, *J*=7.8, 1.0 Hz, 18-H; δ_H7.32 br d, *J*=7.8 Hz, 19-H; δ_C120.67 d, C-16; δ_C120.28 d, C-17; δ_C122.40 d, C-18; δ_C111.02 d, C-19) and an isoprenyl group (δ_H5.91 d, *J*=9.8 Hz, 3-H; δ_H4.80 dm, *J*=9.8 Hz, 21-H; δ_H1.66 d, *J*=0.97 Hz, 23-H; δ_H2.01 d, *J*=0.95 Hz, 24-H; δ_C50.12 d, C-3; δ_C123.77 d, C-21; δ_C25.72 q, C-23; δ_C18.33 q, C-24) together with five quaternary sp^2 carbons (Table 3). The NOEs observed between the former N-H (δ7.91, 1-H) and 19-H (δ7.32) in the 1,2-disubstituted benzene ring in the difference NOE experiments (Table 3) further supported the presence of the indole unit in **3**. Also the ^{1}H and ^{13}C NMR spectra showed signals due to two amide carbonyls (δ171.00 s, C-5 and δ166.13 s, C-11), a hydroxymethine (δ_H5.78 d, *J*=2.9 Hz, 13-H; δ_H4.72 d, *J*=2.9 Hz, 13-O<u>H</u>; δ_C68.66 d, C-13), a hydroxyl proton (δ4.24 br s) and a methine and several methylene groups (Table 3), which could be distributed to the diketopiperazine part in **3** (Table 3) by a comparison of the data with those of **1** and **2** (Table 2). Thus, **3** should be a demethoxy derivative of **1**, constructed by an indole unit, an isoprenyl group and a diketopiperazine moiety like the case of **1** and **2**.

Then those structural units could be confirmed by the results of PFG-HMBC experiments (Table 3) and finally the planar structure of **3** was deduced through connecting those structural units by extensive analysis of the structural information from the PFG-HMBC experiments. The results of NMR studies for **3** are summarized in Table 3.

Cyclotryprostatin D (**4**), an amorphous powder, showed $[\alpha]_D$ +88.0° ($CHCl_3$) and its molecular formula $C_{21}H_{21}N_3O_4$ determined by HR-EI-MS measurement (Table 1) is H_2 less than that of **3**. The UV spectrum of **4** showed absorption maxima at 216 (ε 18290), 240sh (12320), 247 (15310), 264 (9720), 267sh (9570) and 301 nm (8550), which could be distributed to the indole chromophore with a conjugated carbonyl group in **4** by a comparison with the data of **3**. The IR spectrum of **4** suggested, like that of **3**, the presence of a diketopiperazine system in **4** and showed an additional absorption at 1695 cm^{-1} in the functional group region, which could be ascribed to the conjugated carbonyl in **4** (Table 1).

The ^{1}H and ^{13}C NMR spectra (Table 3) of **4** were similar to those of **3**, but they were characterized by the disappearance of signals due to the hydroxymethine group (δ_H5.78 d, *J*=2.9 Hz, 13-H; δ_H4.72 d, *J*=2.9 Hz, 13-O<u>H</u>; δ_C68.66 d, C-13) in **3** and the appearance of a new ^{13}C signal (δ182.02, C-13) assignable to the conjugated carbonyl in **4**, accompanied with slight changes of several proton and carbon signals (Table 3).

The direct comparison of the ^{1}H and ^{13}C NMR spectra with those of **3** (Table 3), coupled with the structural information from the elemental composition and the UV and IR spectra of **4**, led us to consider that **4** may be a 13-oxo derivative of **3**. Eventually the structure of **4** could be determined by detailed analyses of its ^{1}H

Table 3. 500 MHz ^1H and 125 MHz ^{13}C NMR data for **3** and **4** in chloroform-*d*[a)]

Positions	**3**				**4**			
	δ_H (*J* in Hz)	NOEs[b)]	δ_c	HMBC[c)]	δ_H (*J* in Hz)	NOEs[b)]	δ_c	HMBC[c)]
1 (NH)	7.91 br s	3, 19	--------		8.96 br s	3, 19	--------	
2	-----		131.46 s	1,3,13,13-OH[d)]	-----		148.37 s	3
3	5.91[e)] d (9.8)	1, 21, 24	50.12 d		5.90 d (9.0)	21, 24	49.30 d	
5	-----		171.00 s	3, 6, 7β	-----		173.05 s	6[f)], 7β
6	4.42 dd (10.0, 7.1)	7α	58.72 d	7α[d)], 7β, 8β	4.71 dd (8.3, 7.8)	7α	60.16 d	
7α	2.47 m	6, 7β, 8α	29.12 t	6, 9[d)]	2.42 m	6, 7β, 8α	29.06 t	6[f)]
β	2.14-2.02 m				2.10-1.85 m			
8α	1.94 m	7α	22.52 t	7α, 7β	2.10-1.85 m		23.04 t	
β	2.14-2.02 m				2.10-1.85 m			
9	3.63 (2H) m		45.31 t	7α, 8α	3.57 (2H) m		45.60 t	
11	-----		166.13 s	13[d)]	-----		164.87 s	
12	-----		82.99 s	3, 13-OH[d)]	-----		82.70 s	
13	5.78 d (2.9)	13-OH, 21	68.66 d	13-OH	-----		182.02 s	
14	-----		105.41 s	1,3,13,13-OH,16	-----		108.81 s	3[f)]
15	-----		126.38 s	1, 17, 19	-----		123.98 s	16[f)],17[f)],19[f)]
16	7.94 br d (7.8)	17	120.67 d	18	8.11 br d (8.0)		121.98 d	17[f)], 18[g)]
17	7.13 br t (7.8)		120.28 d	18, 19	7.24-7.15 AB type		124.79 d	16, 18
18	7.18 td (7.8, 1.0)		122.40 d	16,19	7.24-7.15 AB type		123.28 s	17[f)], 19[g)]
19	7.32 br d (7.8)	1	111.02 d	17	7.29 br d (7.0)	1	111.56 d	17[g)], 18[g)]
20	-----		136.66 s	1, 16, 18	-----		136.69 s	16, 18[g)]
21	4.80 dm (9.8)	13, 23	123.77 d	3, 23, 24	4.95 br d (9.0)	3, 23	122.29 d	3, 23, 24
22	-----		134.92 s	3, 23, 24	-----		138.18 s	3[g)], 23, 24
23	1.66[h)] d (0.97)	21, 24	25.72 q	21, 24	1.72[h)] s	21, 24	25.78 q	21, 24
24	2.01[i)] d (0.95)	3, 23	18.33 q	21, 23	1.97[i)] s	3, 23	18.63 q	21, 23
12-OH	4.24 br s		--------		undetected		--------	
13-OH	4.72 d (2.9)	13	--------		-----		--------	

a): Signal assignments were based on the results of ^1H-^1H COSY, PFG-HMQC, PFG-HMBC and difference NOE experiments. b): Numbers in the column indicate the protons on where NOEs were observed in the difference NOE experiments under irradiation at the proton in the corresponding line. c): Numbers in the column indicate the protons coupled with the carbon through two, three or four bonds, respectively, which were detected in the PFG-HMBC spectra measured with long-range J_{CH} values of 8.3 or 4 Hz (8 or 16 scans, respectively) for **3** with 12.4 mg sample and 8.3, 5.6 or 5 Hz (48, 128 or 96 scans, respectively) for **4** with 1.2 mg sample, respectively. d): The proton was detected in the PFG-HMBC spectrum measured with a long-range J_{CH} value of 4 Hz (sample 12.4 mg, 16 scans). e): Long-range ^1H-^1H coupling was observed with 13-H in the ^1H-^1H COSY. f) and g): The protons were detected in the PFG-HMBC experiments with the long-range J_{CH} values of 5.6 and 5 Hz (sample 1.2 mg, respective 128 and 96 scans), respectively. h) and i): Long-range ^1H-^1H couplings were observed both with 21-H and with each other, respectively, in each sample in the ^1H-^1H COSYs.

and ^{13}C NMR spectra with the aid of ^{1}H-^{1}H COSY, DEPT, PFG-HMQC and PFG-HMBC techniques and the results were summarized in Table 3.

Stereochemistry of Cyclotryprostatins A (1)-D(4)

The relative stereochemistry for **1-4** shown in Chart 1 could be concluded on the basis of the results of difference NOE experiments (Tables 3 and 4) and the chemical shifts of several proton signals, coupled with the inspection of Draiding model. The stereochemistry around the central heterocyclic and the diketopiperazine rings in **1-4** are reflected mainly in the chemical shifts of 3-H, 21-H, 13-H and 16-H (Tables 3 and 4).

In the difference NOE experiments for **1** and **2**, NOEs were observed between 1-H and 3-H, between 1-H and 19-H, and between 13-H and 16-H, respectively, in both **1** and **2** (Table 2). This indicated that the protons 1-H, 3-H and 19-H and the protons 13-H and 16-H in both **1** and **2** should be in the near planar relations, respectively. Furthermore, in the difference NOE experiment for **2**, irradiation at the protons 13-OCH_3 (δ3.36) caused NOE increase of the 6-H signal at δ4.375 (Table 2). Thus, 13-OCH_3 and 6-H in **2** must be in the *cis*-relation where 13-OCH_3 and 6-H might be near in space with each other, for which 12-OH in **2** should be in the *trans*-relation in contrast to 13-OCH_3 and 6-H as can be seen in Chart 2. The inspection of Draiding model showed that for satisfying the above NOE results, the isoprenyl at C-3 and 12-OH in **2** must be in the same direction and both the central heterocyclic and the diketopiperazine rings in **2** must take half-chair (sofa) conformations with 3-H and 13-H being equatorial and C-21, 6-H, 12-OH and 13-OCH_3 being axial. In this conformation, 1-H, 3-H and 19-H are oriented in the near planar direction and 3-H is also in the another near planar direction with the C-5 carbonyl. Further, 13-H is oriented in the near planar direction with 16-H, while C-21 and 12-OH are in a γ-diaxial relation (Chart 2). This was supported also by the chemical shift (Table 2) of 21-H in **2** which showed a marked down-field shift than those in **3** and **4** (Table 3), which could be explained by the deshielding of the proton by the 12-OH group in **2**. The same stereochemistry for **1** (Chart 2) could be considered reasonably from the close similarity of its NMR data with those of **2** (Table 2).

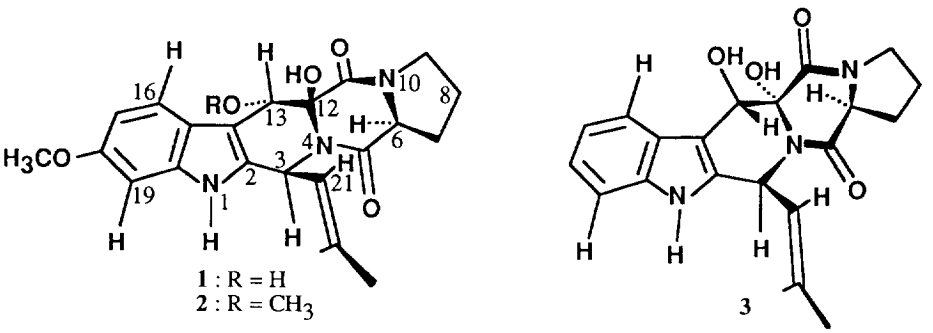

Chart 2 Relative Stereochemistry of **1-3**.

In the difference NOE experiments for **3** and **4**, NOEs were observed between 1-H and 3-H and between 1-H and 19-H, respectively, in both **3** and **4**, and the NOEs between 13-H and 21-H were observed in **3** (Table 3). This indicated the near linear relation between 1-H, 3-H and 19-H in both **3** and **4** and the *cis*-relation

between 13-H and C-21 in **3**, respectively. The inspection of Draiding model showed that for satisfying the above NOE results, the central heterocyclic and the diketopiperazine rings in **3** should respectively take the near boat and boat forms in which 3-H and 13-OH are *quasi*-equatorial and C-21, 6-H, 12-OH and 13-H are *quasi*-axial or axial (Chart 2). In this conformation, 3-H in **3** is in the near planar direction with the protons 1-H and 19-H but not with the C-5 carbonyl, and 13-OH is oriented in the near planar direction with 16-H. Furthermore, the *cis*-1,4-diaxial relations between C-21 and 13-H and between 6-H and 12-OH are required respectively in the opposite side of the pentacyclic ring in **3** (Chart 2), coinciding with the NOEs between 13-H and 21-H. The same stereochemistry at C-3, C-6 and C-12 for **4** could be considered reasonably based on the above NOEs and from the similarity of the chemical shifts of 3-H and 21-H with those of **3** (Table 3), like in the case of **2** and **1**.

The relative stereochemistry for **1**-**4** mentioned above were also supported by the chemical shifts of 3-H, 13-H, 16-H and 21-H (Tables 2 and 3). The protons 3-H (about δ6.65) and 21-H (about δ5.60) in **1** and **2** were deshielded markedly by the C-5 carbonyl and by the 12-OH group, respectively, compared with those in **3** and **4** (about δ5.90 for 3-H in **3** and **4** and δ4.80 in **3** and δ4.95 in **4** both for 21-H). In contrast, the protons 13-H (δ5.78) in **3** and 16-H in both **3** (δ7.94) and **4** (δ8.11) were deshielded by the hydroxyl group at C-13 in **3** and the carbonyl group at C-13 in **4**, respectively, compared with those (Table 2) in **1** and **2**. On the other hand, the down-field shifts of 16-H (δ8.11) and 21-H (δ4.95) in **4** than those in **3** (δ7.94 for 16-H and δ4.80 for 16-H) could be explained in terms of the strong deshielding by the carbonyl group at C-13 for 16-H and the lack of the deshilding by 13-H for 21-H in **4**, respectively, which reflected well the functional change at the C-13 position.

Biological Activities of Cyclotryprostatins A (1) - D (4)

Cell cycle inhibitory activities for **1**-**4** were measured by using mouse tsFT210 cells and the bioassay was carried out by the synchronously cultured assay as we have previously reported[1,4]. The tsFT210 cell line is a temperature-sensitive $p34^{cdc2}$ mutant and the cells grew normally at 32°C, but were arrested in the G2 phase at 39°C. The G2-arrested cells by high temperature synchronously passed through M phase to enter into G1 phase when they were transferred to 32°C. Cyclotryprostatins A (**1**)-D(**4**) inhibited the cell cycle progression of tsFT210 cells at the G2/M phase in the bioassay condition that the G2-arrested cells allowed to pass through M phase to enter into G1 phase by releasing from the temperature-arrest.

Typical flow cytometric histograms for **1**-**4** are given in Fig. 2 and morphological observations of the corresponding cells are also given. Cyclotryprostatin A (**1**)-D (**4**) completely inhibited the cell cycle progression of tsFT210 cells in the G2/M phase at concentrations over 15.2 μM for **1**, 29.4 μM for **2**, 54.1 μM for **3** and 66.0 μM for **4**, respectively, like as shown in Fig. 2. Half maximal inhibitory concentrations (IC_{50}'s) of **1**-**4** were 5.6 μM for **1**, 19.5 μM for **2**, 23.4 μM for **3** and 25.3 μM for **4**, respectively.

DISCUSSIONS

The present work has provided four new natural diketopiperazine derivatives, cyclotryprostatins A (**1**)-D (**4**), as new G2/M phase inhibitors of the mammalian cell cycle.

Cyclotryprostatins A (**1**)-D (**4**) have a pentacyclic ring skeleton involved a 2,5-diketopiperazine ring, which is composed from a tryptophan unit, a proline residue and an isoprenyl group. Up to date, it is the first time to isolate **1**-**4** from a natural source even many natural diketopiperazine derivatives belonging to the same class, such as fumitremorgins, verruculogen and its derivatives, have been reported[12-15], and **2** and **4** are new

compounds discovered for the first time by tracing their cell cycle inhibitory activities in the present study. Furthermore, cyclotryprostatin D (**4**), unique in carrying a ketocarbonyl at C-13, provides the first example of 13-oxo compound of the diketopiperazine derivatives belonging to the same class[16], even a lot of 13-*O*-substituted derivatives of this class have been known[12-16].

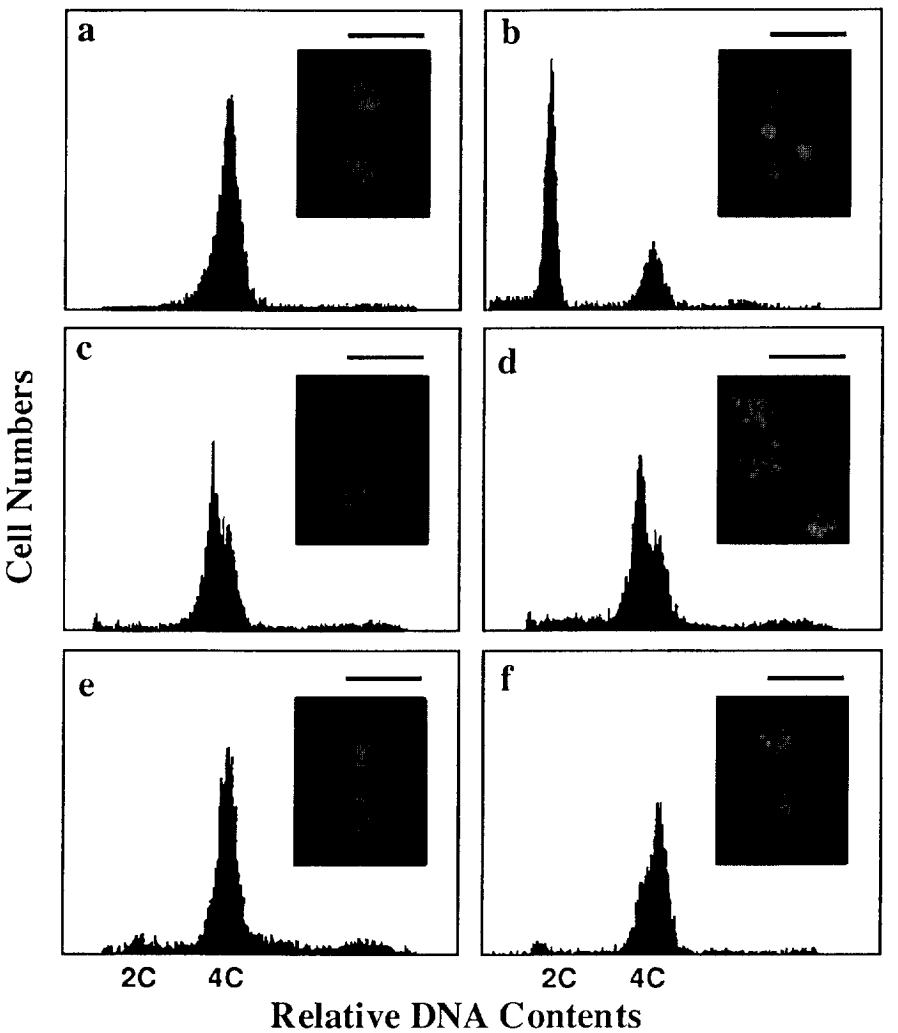

Fig. 2. Effects of **1-4** on the Cell Cycle Progression of tsFT210 Cells.

tsFT210 cells at a density of $2x10^5$ cells/ml in RPMI-1640 medium supplemented with 5% calf serum were synchronized in the G2 phase by incubation at 39.4°C for 17 hours (a). Then the cells were transferred to 32°C for 4 hours in the absence (b) or in the presence of 15.2 μM of **1** (c), 29.4 μM of **2** (d), 54.1 μM of **3** (e), and 66.0 μM of **4** (f), respectively. Photographs show morphological characteristics of the corresponding cells observed under the fluorescence microscope after visualizing the cell nuclei by stain with Heochst 33258 reagent (Bar = 23 μm).

On the other hand, **1** and its *cis*- and *trans*-12,13-isomers as well as **3** and its two *trans*-12,13-isomers were prepared by Kodato *et al* during the synthesis of fumitremorgin B[16]. But the data reported for the title compounds (UV, EI-MS and ^{1}H NMR for **1**; UV, IR and ^{1}H NMR for **3**) and their isomers are not enough to simply identify **1** and **3** by a direct comparison with those of natural compounds. However, the limited data in the literature[16], especially the ^{1}H NMR data, are well agreed with those reported in this paper, evidencing the stereochemistry deduced for **1** and **3** and thus also for **2** and **4** in the present study.

To the cell cycle progression of tsFT210 cells, **1-4** showed an inhibitory activity with the IC_{50} values in the same micromolar order as that for tryprostatins A (78.8 μM)[4] and B (18.8 μM)[4], fumitremorgin C (14.0 μM)[4], demethoxyfumitremorgin C (1.78 μM)[4] and spirotryprostatin B (14.0 μM)[7]. Previously we have reported[4,7] that the methoxy group on the benzene ring in tryprostatin A, spirotryprostatin A and fumitremorgin C negatively dominated the cell cycle inhibitory activity for those compounds, compared with their demethoxy derivatives, tryprostatin B, spirotryprostatin B and demethoxyfumitremorgin C, respectively. The same is true that cyclotryprostatin C (**3**) showed stronger inhibitory activity (IC_{50}=23.4 μM) than that (IC_{50} > 243 μM)[4] of its 18-methoxy derivative 12α,13α-dihydroxyfumitremorgin C (DHFT-C). Cyclotryprostatin A (**1**) is a 12-epimer of DHFT-C, but its inhibitory effect (5.6 μM) was dramatically enhanced than that of DHFT-C (IC_{50} > 243 μM) and was also stronger than that (IC_{50}=23.4 μM) of **3** which is less the methoxy at C-18 and different in the stereochemistry at C-12 than those of **1** (Chart 1). On the other hand, a little change was observed in the inhibitory effects between **3** (23.4 μM) and **4** (25.3 μM), the structures of which were different only at the C-13 position (Chart 1). Those observations suggested an important role of the stereochemistry at C-12 in **1-4**, which resulted in the conformational changes of the central and the diketopiperazine rings in **1-4**, in the inhibitory effects of those compounds on the cell cycle progression of mammalian cells at the G2/M phase. Also, the above results showed that the negative effect of methoxy group on the benzene ring in the related compounds having the pentacyclic ring skeleton should be limited in those with the 12α-proton or 12α-hydroxyl group.

In morphological observations, most portion of the tsFT210 cells treated by **1** and **2** showed morphological characteristics of the condensed chromosomes (Fig. 2, c and d), which are typical of the M phase cells, and a little portion appeared with morphological characteristics of the G2 phase cells (Data could not shown on the photographs in Fig. 2 for **1** and **2**). In contrast, the tsFT210 cells treated by **3** and **4** showed both M and G2 phase morphological characteristics (Fig 2, e and f), but the G2 phase cells occupied the most portion in those cells. This means that the tsFT210 cells treated by **1-4** are trapped both in G2 and M phases, but the main inhibitory points for **1-4** are little different, the M phase for **1** and **2** and the G2 phase for **3** and **4**, respectively. Incidently, the portion of G2 cells are increased dose-dependently in the tsFT210 cells treated by **1-4**, especially in the cells treated by **3** and **4** (data not shown).

Detailed studies on their action mechanisms are currently being undertaken.

EXPERIMENTAL SECTION

General Instrumental Analyses

Melting point was measured using a Yanagimoto micro melting point apparatus and were uncorrected. Optical rotations were determined in $CHCl_3$ solutions on a JASCO DIP-370 polarimeter. UV spectra were taken with a Hitachi 220A spectrophotometer in MeOH solutions and IR spectra were recorded on a Shimadzu FTIR-8100M Fourier transform infrared spectrophotometer in KBr discs. EI-MS (ionization voltage, 70 eV,

accelerating voltage, 3kV) and HR-EI-MS were measured respectively on Hitachi M-80A and Hitachi M-80 mass spectrometers using a direct inlet system. ^{1}H and ^{13}C NMR spectra were taken on a JEOL GSX-500 or α-400 spectrometer with tetramethylsilane as an internal standard and chemical shifts are recorded in δ values. Multiplicities of ^{13}C NMR signals were determined by the DEPT method and are indicated as s (singlet), d (doublet), t (triplet) and q (quartet). 2D NMR spectra (^{1}H-^{1}H or PFG ^{1}H-^{1}H COSY, PFG-HMQC and PFG-HMBC spectra) were measured on a JEOL GSX-500 or α-400 spectrometer by the use of JEOL standard pulse sequences and collected data were processed by JEOL standard software. Difference NOE spectra were obtained by the use of a JEOL standard pulse sequence with irradiation for 5 seconds.

Conditions for Isolation of the Cyclotryprostatins

TLC was done on pre-coated silica gel 60 F_{254} plates (0.25 mm thick, 20 x 20 cm, Merck) and the spots were detected under UV lights (254 and 365 nm) or by the use of 10% aqueous sulfuric acid reagent. Silica gel 60 (230-400 mesh, Merck) was used for column chromatography.

Analytical HPLC was carried out on a reversed phase column (CAPCELL PAK C-18 or C-8, 4.6 x 250 mm, Shiseido Co., Japan) by the use of a HPLC equipment with a Hitachi L-6000 pump and a Waters 991J photodiode array detector system under a flow rate of 1 ml/min. Preparative HPLC was performed on a HPLC system equipped with a Hitachi L-6000 pump and a SSC UV detector under a flow rate of 10 ml/min. CAPCELL PAK C-18 and C-8 columns (20 x 250 mm, Shiseido) were used in the preparative HPLC.

Fermentation of the Producing Fungal Strain

The producing fungal strain, *Aspergillus fumigatus* BM939, on a potato dextrose agar slant was inoculated into a 500-ml cylindrical flask containing 100 ml of the seed medium consisting of glucose 3%, soluble starch 2%, soybean meal 2%, K_2HPO_4 0.5%, $MgSO_4 \cdot 7H_2O$ 0.05% (adjusted to pH 6.5 prior to sterilization) and cultured at 28°C for 27 hours on a rotary shaker at 300 rpm. The culture was transferred into 18 liters of the seed medium with 0.05% of antifoam reagents CA-123 and KM-68, respectively, in a 30-liter jar fermenter. Further fermentation for seed culture was carried out at 28°C for 24 hours with an agitation rate of 350 rpm and an aeration rate of 9 liters/minute.

Then the producing fermentation was carried out in a 600-liter jar fermenter containing 400 liters of the production medium having the same composition of the seed medium with 0.05% of antifoam reagents CA-123 and KM-68, respectively. The seed culture (18 L) was transferred into the 600-liter fermenter and the fermentation was performed at 28°C for 66 hours with an agitation rate of 350 rpm and an aeration rate of 200 liters/min.

Separation of the Fermentation Broth

The whole broth was filtrated to separate into a broth supernatant (370 L) and a mycelial cake. The former was extracted once with 400 L of EtOAc to give an EtOAc solution and the latter was extracted with 90% aqueous acetone (400 L x 1 time) which was evaporated *in vacuo* to remove acetone to give an aqueous solution (60 L). The aqueous solution was extracted with EtOAc (120 L x 2 times) to afford 240 L of EtOAc solution. Both the EtOAc solutions obtained were combined and concentrated *in vacuo* to give an oily extract (1.2 L). To the oily extract, 1.2 L of *n*-hexane was added, and the extract was suspended by stirring followed by sonication for 10 minutes and then the *n*-hexane-insoluble part was obtained by centrifugation at 6000 rpm for 20 minutes. The *n*-hexane-insoluble part was treated two more times with *n*-hexane (1.2 L x 2) by the same manner to remove nonpolar oil fraction. To the *n*-hexane-insoluble part obtained, $CHCl_3$ (1.2 L) was added, sonicated for

10 minutes and then centrifuged for 20 minutes at 6000 rpm to obtain a $CHCl_3$ solution. The $CHCl_3$-insoluble part was extracted one more time with $CHCl_3$ (1.2 L) by the same manner, and both the $CHCl_3$-solutions obtained were combined and concentrated under reduced pressure to afford a $CHCl_3$-soluble syrup. This was treated once more with *n*-hexane (1.2 L) as described above to give a *n*-hexane-insoluble part which was partitioned between $CHCl_3$-H_2O. The $CHCl_3$ solution obtained was concentrated under reduced pressure to give an active $CHCl_3$ extract (66 g) as powders.

The $CHCl_3$ extract (66 g) was dissolved in 250 ml of *n*-hexane-$CHCl_3$ (20:80) solution and subjected to a silica gel column packed in *n*-hexane (silica gel, 1500 g; bed volume, 7.5 x 75 cm; retention volume, 3 L). The column was then eluted successively with *n*-hexane-$CHCl_3$ [50:50 (7.5 L)→ 25:75 (13.7 L)→ 10:90 (9.5 L)] solution, $CHCl_3$ (1.2 L) and $CHCl_3$-MeOH [99.5:0.5 (9 L)→ 99:1 (1.2 L)→ 98:2 (6 L)→ 96:4 (9 L)→ 90:10 (9 L)→ 80:20 (10 L)→ 70:30 (6 L)] solution, respectively. After elution with 7.5 L of *n*-hexane-$CHCl_3$ (50:50) solution which was collected in a portion, the eluate was collected in each 3 L portion, monitored by TLC, combined and concentrated *in vacuo* to give twenty five fractions [**Fr.1**, *n*-hexane-$CHCl_3$ (50:50) eluate; **Fr.2-Fr.4**, *n*-hexane-$CHCl_3$ (25:75) eluate; **Fr.5-Fr.6**, *n*-hexane-$CHCl_3$ (10:90) eluate; **Fr.7**, *n*-hexane-$CHCl_3$ (10:90) & $CHCl_3$ eluate; **Fr.8-Fr.10**, $CHCl_3$ eluate; **Fr.11**, $CHCl_3$ & $CHCl_3$-MeOH (99.5:0.5) eluate; **Fr.12-Fr.13**, $CHCl_3$-MeOH (99.5:0.5) eluate; **Fr.14**, $CHCl_3$-MeOH (99.5:0.5 & 99:1) eluate; **Fr.15-Fr.17**, $CHCl_3$-MeOH (99:1) eluate; **Fr.18-Fr.20**, $CHCl_3$-MeOH (98:2) eluate; **Fr.21-Fr.22**, $CHCl_3$-MeOH (96:4) eluate; **Fr.23**, $CHCl_3$-MeOH (96:4 & 90:10) eluate; **Fr.24** $CHCl_3$-MeOH (90:10) eluate; **Fr.25** $CHCl_3$-MeOH (80:20 &70:30) eluate].

Isolation of Cyclotryprostatins A (1)-D (4)

The fraction **Fr.7** (0.76 g) eluted by *n*-hexane-$CHCl_3$ (10:90) and $CHCl_3$ solutions from the silica gel column was treated with MeOH to give a MeOH soluble part which was separated by preparative HPLC on a CAPCELL PAK C-18 column using MeOH-H_2O (60:40) as eluting solvent (detector wave length, 210 nm) to give an active fraction **fr.5** (Rt=13 min, 32 mg). The fraction **fr.5** was further subjected to a HPLC separation on a CAPCELL PAK C-8 column using MeOH-H_2O (40:60) eluting solution (detector wave length, 210 nm) to give **cyclotryprostatin A** (**1**, Rt=19.6 min, 1.0 mg) and **cyclotryprostatin B** (**2**, Rt=65.6 min, 4.4 mg), respectively, both as pale yellow crystalline forms from MeOH solutions.

The fraction **Fr.14** (0.99 g) eluted by $CHCl_3$-MeOH (99.5:0.5 and 99:1) solvents from the silica gel column was separated by preparative HPLC on a CAPELL PAK C-18 column using MeOH-H_2O (60:40) as eluting solvent (detector wave length, 220 nm) to give **cyclotryprostatin C** (**3**, Rt=38.5 min; 12.4 mg) as white needles from MeOH and crude **cyclotryprostatin D** (**4**, Rt=14.2 min) which was further purified by repeated HPLC under the same condition to give 1.2 mg of pure **4** as a pale yellow amorphous powder from a MeOH solution.

Bioassay for Cell Cycle Inhibitory Activity

The tsFT210 cells were routinely maintained at 32°C in RPMI-1640 medium supplemented with 5% calf serum (HyClone Inc., Logan, UT, USA) in the presence of 30 μg/ml of penicillin and 42 μg/ml of streptomycin under a humidified atmosphere of 5% CO_2 and 95% air. The cells were arrested in the G2 phase by incubation at 39.4°C for 17 hours and the cells were allowed to pass through M phase to enter into G1 phase by incubation at 32°C for 4 hours after treatment with the samples. Then distribution of the cells within cell cycle were determined by flow cytometry as we have previously reported[1,4].

ACKNOWLEDGEMENTS

We thank Ms. Tamiko Chijimatsu (RIKEN) for the measurements of PFG-HMBC spectra. This research work was supported in part by a Grant for "Biodesign Research Program" from RIKEN (C.-B. Cui and H. Osada) and a Grant from Ministry of Education, Japan.

REFERENCES AND NOTES

1. Osada, H.; Cui, C.-B.; Onose, R.; Hanaoka, F. *Bioorg. Med. Chem.*, **1996**, in press.
2. Cui, C.-B.; Kakeya, H.; Okada, G.; Onose, R.; Ubukata, M.; Takahashi, I.; Isono, K.; Osada, H. *J. Antibiot.*, **1995**, *48*, 1382-1384.
3. Cui, C.-B.; Ubukata, M.; Kakeya, H.; Onose, R.; Okada, G.; Takahashi, I.; Isono, K.; Osada, H. *J. Antibiot.*, **1996**, *49*, 216-219.
4. Cui, C.-B.; Kakeya, H.; Okada, G.; Onose, R.; Osada, H. *J. Antibiot.*, **1996**, *49*, 527-533.
5. Cui, C.-B.; Kakeya, H.; Osada, H. *J. Antibiot.*, **1996**, *49*, 534-540.
6. Cui, C.-B.; Kakeya, H.; Osada, H. *J. Antibiot.*, **1996**, *49*, 832-835.
7. Cui, C.-B.; Kakeya, H.; Osada, H. *Tetrahedron*, **1996**, *52*, 12651-12666.
8. In the UV spectra, both the 6-*O*-methylindole and the indole chromophores show a strong absorption in the 220-230 nm region. While in the 250-320 nm region, two major absorption bands like the humps of a camel are typical of the 6-*O*-methylindole chromophore and the appearance of a major one in the same region is characteristic for the indole chromophore, respectively (*cf.* reference 2 and see Cole, R. J.; Cox, R. H. *Handbook of Toxic Fungal Metabolites*, Academic Press Inc.: New York, **1981**; pp. 357-383 for the 6-*O*-methylindole chromophore, pp. 390 and pp. 453-462 for the indole chromophore).
9 Fayos, J.; Lokensgard, D.; Clardy, J.; Cole, R. J.; Kirksey, J. W. *J. Am. Chem. Soc.*, **1974**, *96*, 6785-6787.
10. Steyn, P. S. *Tetrahedron*, **1973**, *29*, 107-120.
11. Steyn, P. S. *Tetrahedron Lett.*, **1971**, 3331-3334.
12. Steyn, P. S.; Vleggaar, R. *Progress in the Chemistry of Organic Natural Products* (Founded by Zechmiester, L.; Edited by Herz, W.; Grisebach, H.; Kirby, G. W.), **1985**, *48*, 1-80.
13. Abaraham, W.-R.; Arfmann, H.-A. *Phytochem.*, **1990**, *29*, 1025-1026.
14. Yamazaki, M.; Fujimoto, H.; kawasaki, T. *Chem. Pharm. Bull.*, **1980**, *28*, 245-254.
15. Cole, R. J.; Cox, R. H. *Handbook of Toxic Fungal Metabolites*, Academic Press Inc.: New York, **1981**; pp. 355-385.
16. Kodato *et al* have recorded that in a mixture of the synthetic mediates for fumitremorgin B, the presence of a 13-ketocarbonyl compound having the same structural skeleton as that in **4** was revealed by the UV absorption at 294.5, 269.5 and 308 nm, corresponding to the 3-acylindole chromophore, in the UV spectrum of the mixture in an EtOH solution. But they did not isolate the compound in a pure form. Kodato, S.; Nakagawa, M.; Hongu, M.; Kawata, T.; Hino, T. *Tetrahedron*, **1988**, *44*, 359-377.

(*Received in Japan* 26 *August* 1996; *accepted* 21 *October* 1996)